Contribution from the Department of Chemistry,
University of Houston, Houston, Texas 77004

Polyaza Cavity-Shaped Molecules. 12. Ruthenium(II) Complexes of 3,3′-Annelated 2,2′-Bipyridine: Synthesis, Properties, and Structure

Randolph P. Thummel,* Francois Lefoulon, and James D. Korp

Received November 13, 1986

Ruthenium(II) complexes of the types $RuL_3(PF_6)_2$ and $Ru(bpy)_2L(PF_6)_2$ have been prepared where bpy = 2,2′-bipyridine and L is a 3,3-′polymethylene-bridged derivative of 2,2′-bipyridine. Analysis of the NMR chemical shifts of H_4, H_5, and H_6 provides insight into the conformation of the complex as well as the strength of the coordinative bond. The absorption and emission energies of these complexes are quite similar to those of $Ru(bpy)_3^{2+}$, while the emission intensities for complexes with highly distorted ligands are diminished. The oxidation potentials of the tris complexes, $RuL_3(PF_6)_2$, shift to more negative potential with increasing length of the polymethylene bridge. An X-ray structure has been determined for the complex $Ru(bpy)_2(\mathbf{4d})[PF_6]_2$ with the molecular formula $C_{34}H_{32}F_{12}N_6OP_2Ru$, which crystallizes in the space group $P\bar{1}$ with two molecules per unit cell and a = 12.485 (3) Å, b = 12.492 (7) Å, c = 12.563 (3) Å, α = 96.91 (3)°, β = 109.80 (2)°, and γ = 90.44 (3)°. Of the two diastereomers possible for the complex, only one is detected, indicating that the Δ form of the metal preferentially coordinates with the D form of **4d** (**4d** = 3,3′-tetramethylene-2,2′-bipyridine) and the Λ form of the metal coordinates with the L form of **4d**. Substantial nonplanarity of the pyridine rings is observed.

Introduction

Recent interest in the properties of ruthenium(II) complexes of bipyridine-type ligands[1] has centered around their photophysical and redox properties with particular emphasis on the electron-transfer processes involved in the photochemical decomposition of water.[2] Attempts have been made to modify the properties of these complexes by altering the steric and electronic character of the ligand.[3] In this paper we report our investigation of how the conformational properties of bipyridine ligands influence their ruthenium(II) complexes.

We have recently prepared the series of 3,3′-annelated 2,2′-bipyridines (**1**).[4] The length of the annelating bridge controls

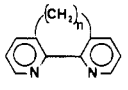

1a n = 1
b n = 2
c n = 3
d n = 4

both the dihedral angle between the pyridine rings and the distance between the two nitrogen lone pairs. We reasoned that these two interrelated characteristics should strongly influence the coordination properties of the ligand. By NMR systems **1b** and **1c** are conformationally mobile at room temperature, while **1d** is conformationally rigid, showing four distinct signals in its ^1H NMR spectrum. Thus **1d** is capable of conformational enantiomerism, and the transition state for racemization would have the two pyridine rings coplanar, which is presumably their optimum geometry for octahedral coordination.

A recent report from Cherry and co-workers on the ruthenium(II) complexes of 4,5-diazafluorene (**1a**) claims that the monomethylene bridge of **1a** distorts the bipyridine portion of the molecule so as to produce a weaker σ-bonding ligand.[5] This property of **1a** results in a lower energy ligand field (LF) state for its ruthenium complexes and consequently a very low intensity emission at room temperature due to preferential population of this LF state, which efficiently decays by a nonradiative process.

Zelewsky and Belser have prepared a series of 3,3′-annelated biquinoline analogues of **1a–c** with either methyl or phenyl substituents in the 4- and 4-′positions (**2a–c**).[3h] Although the ruthenium complexes of these ligands also evidence modified properties when compared with $Ru(bpy)_3^{2+}$, two factors, in addition to ligand conformation, must be taken into consideration in accounting for this behavior. First, the biquinoline nucleus is more delocalized than bipyridine, leading to lower energy metal to ligand charge transfer (MLCT) states. Second, the two fused benzo rings significantly increase steric crowding in octahedral complexes, especially of the tris variety, leading to effects resulting primarily from congestion.

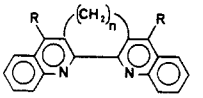

2a n = 1 (R = CH_3 or C_6H_5)
b n = 2
c n = 3

Primarily on the basis of the results from these two groups, we undertook a study of the ruthenium(II) complexes derived from ligands **1b–d** wherein we should be more readily able to directly assess the effect of bipyridine conformation on the coordination geometry and other properties of the system.

Synthesis

The preparation of the ligands **1a–d** has been reported previously.[4] The tris complexes of the type RuL_3^{2+} were prepared by reacting $RuCl_3$ with excess ligand in aqueous ethanol and precipitating the complex by the addition of NH_4PF_6. Purification

$$\mathbf{1a\text{–}d} + RuCl_3\cdot 3H_2O \xrightarrow{NH_4PF_6} RuL_3(PF_6)_2$$

3a, L = **1a** (61%)
3b, L = **1b** (36%)
3c, L = **1c** (58%)
3d, L = **1d** (62%)

was effected by chromatography on alumina eluting with toluene/acetonitrile followed by crystallization of the complex from

(1) See for example: (a) Watts, R. J. *J. Chem. Educ.* **1983**, *60*, 834. (b) Seddon, E. A.; Seddon, K. R. *The Chemistry of Ruthenium*; Elsevier: New York, 1984; Chapter 9. (c) Kalyanasundaram, K. *Coord. Chem. Rev.* **1982**, 159. (d) Durham, B.; Caspar, J. V.; Nagle, J. K.; Meyer, T. J. *J. Am. Chem. Soc.* **1982**, *104*, 4803. (e) Creutz, C.; Keller, A. D.; Sutin, N.; Zipp, A. P. *Ibid.* **1982**, *104*, 3618 and references cited therein.

(2) See for example: (a) Abruna, H. D.; Teng, A. Y.; Samuels, G. J.; Meyer, T. J. *J. Am. Chem. Soc.* **1979**, *101*, 6745. (b) Lehn, J.-M.; Sauvage, J.-P.; Ziessel, R. *Nouv. J. Chim.* **1979**, *3*, 423. (c) Juris, A.; Barigelletti, F.; Balzani, V.; Belser, P.; von Zelewsky, A. *Isr. J. Chem.* **1982**, *22*, 87. (d) Connolly, J. S. *Photochemical Conversion and Storage of Solar Energy*; Academic: New York, 1981; Chapters 4 and 5 and references therein.

(3) (a) Thummel, R. P.; Lefoulon, F. *Inorg. Chem.* **1987**, *26*, 675. (b) Thummel, R. P.; Decloitre, Y.; Fefoulon, F. *Inorg. Chim. Acta* **1987**, *128*, 245. (c) Binamira-Soriga, E.; Sprouse, S. D.; Watts, R. J.; Kaska, W. C. *Inorg. Chim. Acta* **1984**, *84*, 135. (d) Klassen, D. M. *Inorg. Chem.* **1976**, *15*, 3166. (e) Anderson, S.; Seddon, K. R.; Wright, R. D. *Chem. Phys. Lett.* **1980**, *71*, 220. (f) Allen, G. H.; White, R. P.; Rillema, D. P.; Meyer, T. J. *J. Am. Chem. Soc.* **1984**, *106*, 2613. (g) Balzani, V.; Juris, A.; Barigelletti, F.; Belser, P.; von Zelewsky, A. *Sci. Pap. Inst. Phys. Chem. Res. (Jpn.)* **1984**, *78*, 78. (h) Belser, P.; von Zelewsky, A. *Helv. Chim. Acta* **1980**, *63*, 1675. (i) Belser, P.; von Zelewsky, A. *Chem. Phys. Lett.* **1982**, *89*, 101.

(4) Thummel, R. P.; Lefoulon, F.; Mahadevan, R. *J. Org. Chem.* **1985**, *50*, 3824.

(5) Henderson, L. J.; Fronczek, F. R.; Cherry, W. R. *J. Am. Chem. Soc.* **1984**, *106*, 5876.

0020-1669/87/1326-2370$01.50/0

Table I. Proton NMR Chemical Shift Data[a] for RuL_3^{2+} Complexes and the Corresponding Ligands

substrate	H_3	H_4	H_5	H_6	$-CH_2-$
$Ru(bpy)_3^{2+}$	8.53	8.06	7.41	7.75	
bpy	8.42	7.78	7.36	8.65	
$\Delta\delta$	+0.11	+0.28	+0.05	−0.90	
3a		8.10	7.43	7.83	4.40
1a		7.96	7.34	8.65	3.88
$\Delta\delta$		+0.14	+0.09	−0.82	+0.52
3b		7.77	7.29	7.55	3.25
1b		7.60	7.24	8.56	2.93
$\Delta\delta$		+0.17	+0.05	−1.01	
3c		7.80	7.20	7.68	2.87/2.51
1c		7.67	7.34	8.61	2.46/1.94
$\Delta\delta$		+0.13	−0.14	−0.93	
3d		7.75	7.17	7.75	1.8–2.9
1d		7.68	7.37	8.51	1.5–2.8
$\Delta\delta$		+0.07	−0.20	−0.76	

[a] Obtained at 300 MHz in CD_3CN and reported in ppm downfield from internal Me_4Si.

the concentrated eluent. The mixed-ligand complexes, $Ru(bpy)_2L^{2+}$, were prepared in a similar manner using *cis*-$Ru(bpy)_2Cl_2$ in place of $RuCl_3$. The yields for all the complexes,

$$\textbf{1a–d} + Ru(bpy)_2Cl_2 \xrightarrow{NH_4PF_6} Ru(bpy)_2L(PF_6)_2$$

4a, L = **1a** (63%)
4b, L = **1b** (59%)
4c, L = **1c** (67%)
4d, L = **1d** (53%)

except **3b**, were in the range of 53–67%, which does not indicate any particular problems with complex formation. No attempt was made to optimize the yield of **3b**.

All complexes were soluble in CD_3CN and thus were characterized by their 300-MHz ^1H NMR spectra. High symmetry allowed complete assignment of the RuL_3^{2+} complexes, and these data are collected in Table I. In the mixed-ligand complexes, $Ru(bpy)_2L^{2+}$, there are 14 nonequivalent aromatic protons causing the downfield region to become too complex for complete assignment. The 3,3′-bridge protons appeared at higher field and integrated correctly for the reported stoichiometry. All new compounds gave satisfactory elemental analyses.

Properties and Conformational Effects

NMR Spectra. Constable and Lewis have carried out a careful study of the ^1H NMR spectrum of $Ru(bpy)_3(BF_4)_2$ in acetone-d_6 at 400 MHz.[6] By utilizing methyl-substituted derivatives of bpy and examining relaxation behavior, they have unambiguously assigned the four aromatic resonances for this complex. For $Ru(bpy)_3(PF_6)_2$ in CD_3CN at 300 MHz we observe a very similar pattern solvent shifted upfield by about 0.2–0.3 ppm. For the symmetrical complexes of our annelated ligands, RuL_3^{2+}, the resonance for H_3 (and $H_{3'}$) disappears and we now observe H_4 (and $H_{4'}$) as the lowest field signal, a doublet of doublets with J_{ortho} = 7.8 Hz and J_{meta} = 1.4 Hz.

Several well-defined and significant trends are apparent for the aromatic protons of the tris complexes **3**. For H_4, complexation leads to a downfield shift of 0.07–0.17 ppm. This proton is the most remote from the other ligands and thus experiences primarily a deshielding effect due to charge depletion resulting from formation of the coordinative bond. The smallest shift is observed for **3d** (0.07 ppm), in which the ligand is the most distorted from planarity, leading to weaker bonding to ruthenium. The greatest downfield shift is observed for the parent system, $Ru(bpy)_3^{2+}$, in which the ligand can readily adopt the optimum conformation for binding and thus form the strongest coordinative bond.

In the uncoordinated ligand, H_6 is the lowest field resonance due to a combination of inductive and resonance deshielding at this position. These effects are overridden in the ruthenium complex, however, and this proton moves substantially upfield as a result of its being pointed directly toward the shielding face of a pyridine ring of the orthogonal ligand (see Figure 1). The magnitude of this shift varies considerably (−0.76 to −1.01 ppm) and may be taken as a sensitive measure of the conformation of the coordinated ligand. For $Ru(bpy)_3^{2+}$ the value of −0.90 ppm indicates a planar ligand in an unstrained orthogonal arrangement around ruthenium. For **3b,c**, flattening of the ligand to achieve planarity increases the angle α due to torsional effects in the polymethylene bridge. This distortion results in H_6 being pushed deeper into the shielding face of the orthogonal pyridine ring, causing it to resonate at higher field. This effect is mediated somewhat for **3c** by twisting about the 2,2′-bond, which directs H_6 somewhat away from this shielding region. The effect of nonplanarity in the ligand is most apparent for **3d**, where the upfield shift is only −0.76 ppm.

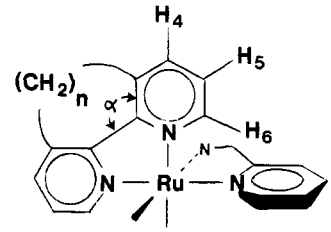

Figure 1. Partial structure of an octahedral ruthenium complex showing the stereochemical relationship of the orthogonal ligands.

The monomethylene-bridged system **3a** also evidences less shielding of H_6 although it is the most planar ligand. In this case the short bridge pulls the two pyridine rings together, decreasing α and drawing H_6 away from the shielding face of the orthogonal bipyridine.

The proton H_5 lies approximately along the axis of the bond joining the two pyridine rings and thus is less sensitive to conformational changes resulting in nonplanarity of the ligand. On the other hand, it is still sensitive to bending of the 2,2′-bond, and thus as α increases for the coordinated ligand (as one proceeds along the series **3a–d**), H_5 is pushed closer to the shielding face of the adjacent pyridine and its shift to higher field increases.

A second important aspect of the NMR spectra for both series of complexes is the conformation of the polymethylene bridge. We have stated that planarity of the bipyridine portion of **1b–d** would correspond to the transition-state conformation for racemization of these systems. Since coordination appears to have a flattening effect upon the ligand, we might expect a lower barrier for conformational inversion in the coordinated ligand. On the other hand, the five-membered-ring metallacycle portion of the complex represents a second bridge between the halves of bipyridine and would thereby impose greater constraints on conformational mobility.

As expected, both the mixed and tris complexes of the monomethylene-bridged system **3a** and **4a** show a singlet for the bridge protons due to the rigid, planar nature of this ligand. The dimethylene-bridged complexes **3b** and **4b** also show a singlet for the bridge protons, indicating that the complexed ligand is still conformationally mobile on the NMR time scale. This is in contrast to the previously reported complex RuL_3^{2+} where L is 3,3′-dimethylene-2,2′-biquinoline, in which the bridge protons showed nonequivalence due to a lack of conformational mobility.[3a,h] In comparison of this biquinoline complex to the corresponding bipyridine one, the congestion caused by the six fused benzo rings must be the cause of the increased inversion barrier. For the tetramethylene-bridged system, the spectra of complexe **3d** and **4d** show that the ligand is conformationally rigid but are too complex for a more detailed analysis.

The trimethylene-bridged system is more readily interpreted. The ligand **1c** is conformationally mobile at room temperature on the NMR time scale, showing a doublet of doublets for the benzylic methylene protons at 2.41 ppm and triplet of triplets for the non-benzylic group at 2.12 ppm. Upon formation of the tris complex, **3c**, the ligand becomes conformationally rigid and the downfield signal splits into two signals at 2.91 and 2.84 ppm. The

(6) Constable, E. C.; Lewis, J. *Inorg. Chim. Acta* **1983**, *70*, 251.

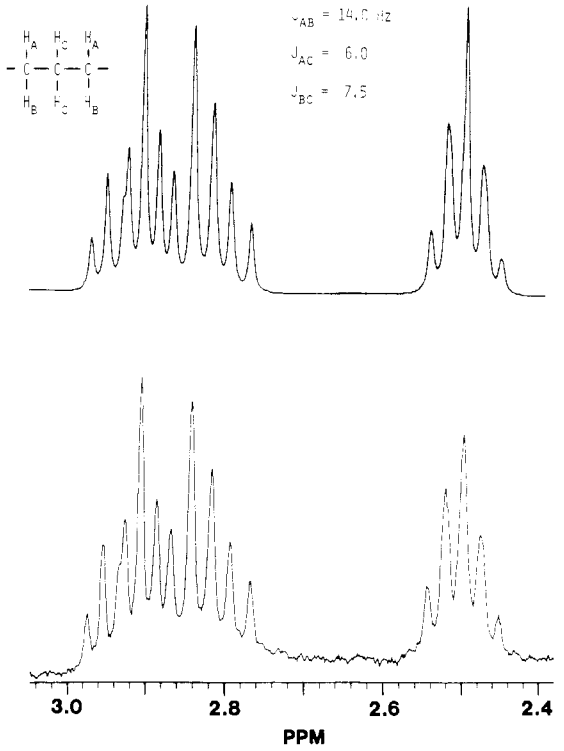

Figure 2. ^1H NMR spectrum of the aliphatic region of **3c**: bottom, experimental spectrum at 300 MHz in CD_3CN; top, simulated spectrum.

Table II. Electronic Absorption Data for Ruthenium Complexes in Acetonitrile (c 5.35 × 10^{-5} M)

complex	λ_{max}, nm (ϵ)			
$Ru(bpy)_3^{2+}$	448 (12 500)	436 (11 400)	284 (71 000)	242 (18 700)
3a	437 (11 800)	424 (10 800)	288 (61 700)	224 (24 300)
3b	452 (13 300)	439 (11 600)	298 (59 800)	215 (29 900)
3c	460 (14 600)	441 (12 700)	294 (69 100)	231 (39 200)
3d	460 (12 100)	440 (10 700)	297 (51 400)	238 (31 800)
4a	446 (13 100)	434 (12 000)	286 (77 600)	240 (15 900)
4b	449 (10 700)	432 (8800)	286 (57 000)	240 (12 100)
4c	453 (10 800)	439 (9300)	288 (73 800)	238 (21 500)
4d	450 (7500)	441 (6900)	286 (58 900)	240 (17 800)

central $-CH_2-$ protons remain equivalent by symmetry and appear at 2.50 ppm, leading to an ABC system that can be simulated to provide the coupling constants given in Figure 2.

Electronic Spectra. The electronic absorption data for complexes **3** and **4** are summarized in Table II. Both species show a band in the region 437–460 nm with a less intense shoulder at shorter wavelength. This absorption is attributed to the MLCT state and is associated with the promotion of a ruthenium d electron into a π^* orbital of the ligand. Cherry and co-workers[5] have noted that the absorption spectrum of **3a** is nearly superimposable with that of $Ru(bpy)_3^{2+}$. We find this similarity in the MLCT absorption to be evident for all the complexes under discussion. It has been reasonably well established that such ruthenium MLCT states are not delocalized over all the ligands but are localized on an individual ligand with a preference for that one having the lowest energy π^* state.[7] We do not observe splitting of the MLCT absorption since for **3** and **4** all three ligands are expected to have π^* energies that are nearly the same.

A more intense band appears in the region 284–298 nm and is associated with a $\pi \rightarrow \pi^*$ absorption of the ligand. This band correlates reasonably well with a similar band observed for the free ligands in the range 268–313 nm. For the ligands, this band steadily shifts to shorter wavelength with increasing length of the annelating bridge and concurrent increase in the bipyridine dihedral angle. The ruthenium complexes **3** do not shown this trend

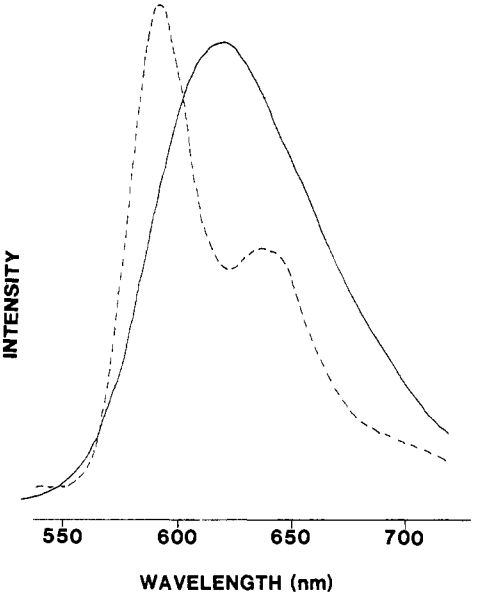

Figure 3. Emission spectrum of **4d** in EtOH–MeOH (4:1) at 77 K (dashed line) and 298 K (solid line).

due to less variation in the dihedral angle between the pyridine rings as a result of coordination. For the mixed-ligand complexes, $Ru(bpy)_2L^{2+}$, we find little difference from the parent system, $Ru(bpy)_3^{2+}$.

The emission spectra of complexes **3b–d** and **4b–d** were recorded at 77 and 298 K, and the results are tabulated in Table III. Our observations for **3b** and **4b** are in good accord with the results of previous workers.[3g] The room-temperature emission spectra of **3b,c** and **4b–d** were quite similar and showed a single band in the region 611–620 nm. Complex **3d** was unusual in that it showed only a very weak emission band at 680 nm. At 77 K the emissions split into a strong and a weak band, as is characteristic of the parent complex. In all cases but **3d**, the position of these two maxima bracketed the values for the room-temperature emission. This temperature-dependent behavior for ruthenium polypyridine complexes has been recently discussed by Balzani and co-workers.[8]

The two systems of greatest interest are the extreme cases involving ligands **1a** and **1d**. The former of these has been examined by Cherry and co-workers.[5] They compare the emission spectra observed for **4a** and $Ru(bpy)_3^{2+}$ at 298 and 77 K. At low temperature the two spectra are quite similar in intensity, while at room temperature there is a drastic reduction in the intensity of **4a** relative to $Ru(bpy)_3^{2+}$. They attribute this difference to more efficient population of the LF state at elevated temperatures. This LF state may then efficiently decay to the ground state via a radiationless process. The lowering in energy of the LF state is ultimately attributed to **1a** being a weaker σ-bonding ligand than bpy due to the increased bite angle caused by monomethylene bridging.

The same arguments set forth by Cherry can be invoked to explain the behavior of complexes **3d** and **4d**. Although the chelating pocket of **1d** is highly distorted by tetramethylene bridging, coordination modifies this effect in a manner that is not possible for **1a**, whose shape changes very little upon coordination. Thus **1d** may be a stronger σ-bonding ligand than **1a**, and we are able to observe a very weak emission for **3d** at room temperature and a more intense one at 77 K. For the mixed-ligand complex **4d**, emission bands are observed at both 77 and 298 K and are illustrated in Figure 3.

Redox Potentials. Table IV summarizes the half-wave potentials as determined by cyclic voltammetry for the ruthenium(II) complexes under discussion. In every case we observe one reversible oxidation wave and three reversible reductions. The usual criteria for reversability were invoked such that the separation

(7) Reference 1b, Chapter 15.

(8) Barigelletti, F.; von Zelewsky, A.; Juris, A.; Balzani, V. *J. Phys. Chem.* **1985**, *89*, 3680.

Table III. Emission Maxima for Ruthenium Complexes in EtOH–MeOH (4:1) (Irradiated at 500 nm)

complex	λ_{max}(298 K), nm	λ_{max}(77 K), nm	complex	λ_{max}(298 K), nm	λ_{max}(77 K), nm
$Ru(bpy)_3^{2+}$	603[a]	578[b]	**4a**	*b*, *c*	574[b]
3a	*b*, *c*	585[b] (vw)	**4b**	611	585 (628 sh)
3b	611	586 (627 sh)	**4c**	615	595 (640 sh)
3c	620 (540 sh)	598 (656 sh)	**4d**	618	590 (637 sh)
3d	680 (vw)	601 (647 sh)			

[a] Harriman, A. *J. Chem. Soc., Chem. Commun.* **1977**, 777. [b] Reference 5. [c] Too weak to measure.

Table IV. Half-Wave Potentials for Ruthenium(II) Complexes[a]

complex	$E_{1/2}$(oxidn)		$E_{1/2}$(redn)	
	Ru^{4+}/Ru^{3+}	Ru^{2+}/Ru^{+}	Ru^{+}/Ru^{0}	Ru^{0}/Ru^{-}
$Ru(bpy)_3^{2+}$	+1.30	−1.33	−1.52	−1.77
3a	+1.30	−1.42	−1.59	−1.82
3b	+1.21	−1.39	−1.57	−1.82
3c	+1.17	−1.37	−1.55	−1.80
3d	+1.17	−1.43	−1.59	−1.84
4a	+1.28	−1.35	−1.55	−1.79
4b	+1.26	−1.34	−1.53	−1.77
4c	+1.26	−1.34	−1.53	−1.77
4d	+1.25	−1.33	−1.53	−1.79

[a] Potentials are in volts vs. SCE, and all waves were reversible. Solutions were 0.1 M in TBAP; the solvent was acetonitrile; $T = 25 \pm 1$ °C.

of the anodic and cathodic peaks, ΔE ($E_p^a - E_p^c$), is equal to or less than 60 mV for a one-electron process and that the ratio of anodic to cathodic currents, i_p^a/i_p^c, is unity.[9] Our values for the oxidation and first reduction potential of **3b** and **4b** are in excellent agreement with the values reported by Balzani and co-workers.[3g]

The mixed-ligand complexes all show oxidation and reduction potentials that fall within a narrow range, differing at most by 0.03 eV and very close to the values for the parent system, $Ru(bpy)_3^{2+}$. Since other mixed-ligand complexes involving more delocalized ligands have shown substantial changes in their electrochemical potentials, the implication is that electronic delocalization effects are more important than conformational ones in determining redox properties. For the tris complexes, **3a–d**, the reduction potentials again fall in a narrow range and no clear trend is obvious. For the oxidation of these same complexes we do observe a shift to more negative oxidation potential with increasing length of the 3,3′-bridge. Since oxidation involves the removal of an electron from a ruthenium t_{2g} orbital, the increasing facility for this process implies higher lying t_{2g} levels. This trend correlates well with the long-wavelength absorptions for these complexes (Table II), where the absorption maxima shift to lower energy with increasing bridge length.

Structural Considerations. It has been noted earlier that **1b–d** are capable of conformational enantiomerism via twisting about the 2,2′-bond leading to the existence of D and L isomers. We have shown that when the inversion barrier for **1c** and **1d** is sufficiently high, the coordinated ligand is not conformationally mobile on the NMR time scale. These facts raise several interesting stereochemical questions regarding complexes **3c,d** and **4c,d**. For the tris complexes **3c,d**, what is the configuration of each of the three complexed ligands? We obtained crystals of both complexes and determined that **3d** has a 3-fold symmetry axis but were unable to obtain a crystallographic solution of the structure. The observed symmetry, however, indicates that all three ligands must have the same absolute configuration.

For the mixed-ligand complexes **4c,d**, the situation is simplified since the two bpy ligands are achiral. These molecules therefore possess only two chiral centers, one due to the bridged ligand and one due to the metal atom. Figure 4 depicts the four possible stereoisomers for the complex $Ru(bpy)_2L^{2+}$. The pair of enantiomers depicted at the top of the figure have the D form of the ligand coordinated to the Λ form of the metal or the L form of the ligand coordinated to the Δ form of the metal. These forms may be interconverted by inversion of configuration at both the ligand and metal centers. If just one center is inverted, the pair of enantiomers shown at the bottom of Figure 4 is produced.

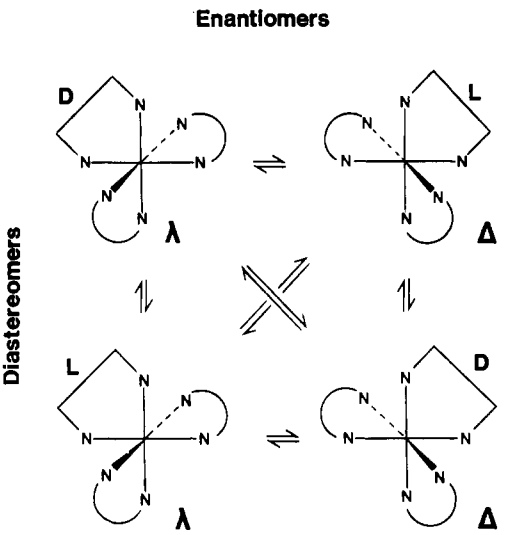

Figure 4. Stereoisomers of ruthenium(II) mixed-ligand complexes. Nitrogens connected by a curved line represent 2,2′-bipyridine, and nitrogens connected by right-angled lines represent a 3,3′-bridged bipyridine.

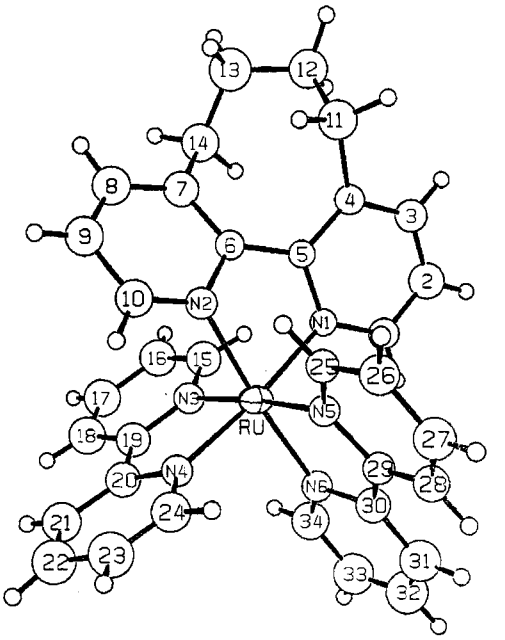

Figure 5. ORTEP drawing of **4d** with atomic numbering scheme.

Careful purification of complex **4d** led to nearly quantitative recovery of crystals, which were analyzed by single-crystal X-ray diffraction. The pertinent geometric features of this complex are given in Table V, while the atomic numbering scheme is included on the ORTEP plot in Figure 5.

It is apparent that the Ru–N bond lengths are relatively unperturbed for the bridged ligand and all six Ru–N bonds are in

(9) Bard, A. J.; Faulkner, L. R. *Electrochemical Methods*; Wiley: New York, 1980; p 227.

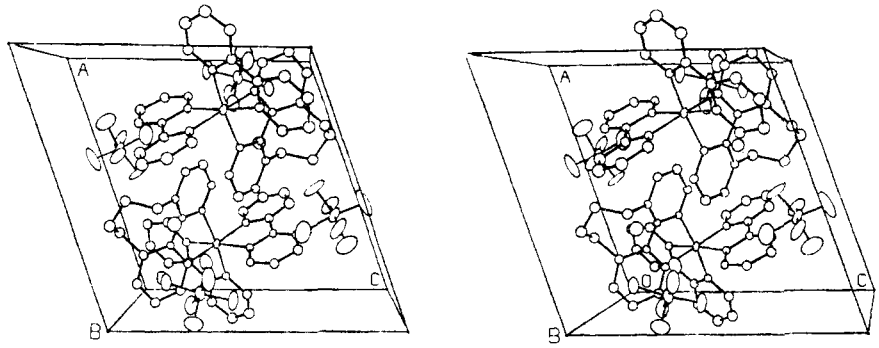

Figure 6. Stereochemical representation of the **4d** unit cell.

Table V. Pertinent Geometric Features of the $Ru(bpy)_2(\mathbf{4d})(PF_6)_2$ Complex

Bond Lengths (Å)			
Ru–N1	2.040 (4)	Ru–N4	2.017 (4)
Ru–N2	2.068 (4)	Ru–N5	2.055 (3)
Ru–N3	2.085 (4)	Ru–N6	2.024 (3)
Bond Angles (deg)			
N1–Ru–N2	79.1	N1–Ru–N4	172.9
N3–Ru–N4	78.7	N2–Ru–N6	174.1
N5–Ru–N6	78.3	N3–Ru–N5	175.6
Torsion Angles (deg)			
1. About the Inter-Pyridine Bond			
N1–C5–C6–N2	25.9	C18–C19–C20–C21	2.9
C4–C5–C6–C7	34.8	N5–C29–C30–N6	−7.2
N3–C19–C20–N4	−1.4	C28–C29–C30–C31	3.5
2. Interior to the Pyridine Rings			
Ligand L			
N1–C1–C2–C3	6.5	N2–C6–C7–C8	12.5
C1–C2–C3–C4	−4.8	C6–C7–C8–C9	−4.0
C2–C3–C4–C5	−5.2	C7–C8–C9–C10	−5.2
C3–C4–C5–N1	14.2	C8–C9–C10–N2	6.4
C4–C5–N1–C1	−12.7	C9–C10–N2–C6	1.9
C5–N1–C1–C2	2.3	C10–N2–C6–C7	−11.6
ω	45.7	ω	41.6
Bpy			
N3–C15–C16–C17	−3.4	N4–C20–C21–C22	0.5
C15–C16–C17–C18	3.9	C20–C21–C22–C23	−0.5
C16–C17–C18–C19	−3.8	C21–C22–C23–C24	0.7
C17–C18–C19–N3	3.1	C22–C23–C24–N4	−0.9
C18–C19–N3–C15	−3.0	C23–C24–N4–C20	0.9
C18–N3–C15–C16	3.3	C24–N4–C20–C21	−0.7
ω	20.5	ω	4.2
Bpy			
N5–C25–C26–C27	−5.8	N6–C30–C31–C32	4.1
C25–C26–C27–C28	5.1	C30–C31–C32–C33	−3.6
C26–C27–C28–C29	−2.7	C31–C32–C33–C34	3.0
C27–C28–C29–N5	0.6	C32–C33–C34–N6	−3.0
C28–C29–N5–C25	−1.3	C33–C34–N6–C30	3.2
C29–N5–C25–C26	4.0	C34–N6–C30–C31	−3.8
ω	19.5	ω	20.7
3. About the Pyridine-Bridge Bond			
C5–C4–C11–C12	−96.7	C6–C7–C14–C13	−101.1

good agreement with the value of 2.056 Å found for $Ru(bpy)_3^{2+}$.[10] The N–Ru–N bond angles are also normal and bracket the value of 78.7° reported for $Ru(bpy)_3^{2+}$. It is noteworthy that the largest bite angle (79.1°) is associated with the tetramethylene-bridged ligand. Cherry has reported an angle of 80.1° for complex **4a**.[5]

The torsion angles about the inter-pyridine bond indicate that the two bpy ligands are relatively planar but the bridged ligand is distorted from planarity. The dihedral angle between the least-squares planes of the two pyridine rings of **1d** is 30.4°. From an examination of molecular models we have estimated the maximum dihedral angle between the pyridine rings of the free ligand **1d** to be about 80°. Thus it appears that substantial flattening of the ligand has occurred as a result of coordination. This flattening results in distortion of the tetramethylene bridge as well as distortion from planarity of the pyridine rings themselves.

Table VI. Yield and Combustion Analysis Data for Ruthenium Complexes

		% calcd			% found		
complex	yield, %	C	H	N	C	H	N
3a	61	44.25	2.68	9.39	44.27	2.71	9.31
3b	36	46.10	3.20	8.96	46.04	3.23	8.91
3c	58	47.80	3.68	8.58	47.59	3.71	8.53
3d	62				*a*		
4a	63	42.71	2.76	9.64	42.85	2.78	9.68
4b	59	43.39	2.94	9.49	43.74	2.98	9.50
4c	67	44.01	3.11	9.34	44.17	3.15	9.31
4d	53				*a*		

[a] Insufficient sample available for analysis.

The relative planarity of the pyridine rings can be evaluated by comparison of their ω values, where ω equals the sum of the absolute values of the six interior torsion angles in the aromatic ring. For a completely planar ring, ω = 0°. From the values of ω summarized in Table V, we can see that the two pyridine rings of the bridged ligand are substantially distorted from planarity.

The crystal structure of **4d** belongs to space group $P\bar{1}$ and is centrosymmetric, containing two molecules in the unit cell (Figure 6). These molecules are enantiomers having the structures corresponding to Δ(D) and Λ(L), as illustrated in the lower half of Figure 4. The structure represented by Figure 5 is the Δ(D) form according to the (+) sign associated with torsion angle C4–C5–C6–C7. The chirality of coordinated **4d** is further supported by the negative sign of the torsion angles associated with the bonds connecting carbons 3 and 3′ to the bridge methylene groups. An inspection of molecular models of both the Δ and Λ forms of $Ru(bpy)_3$ and the D and L forms of **1d** indicates that significant steric interaction with H_6 on the two bpy ligands is avoided when coordination occurs in the fashion Δ(D) and Λ(L). It is tempting to suggest that, in fact, the coordination process is therefore enantioselective. However, the reaction of $Ru(bpy)_2Cl_2$ probably does not occur in a concerted fashion,[11] and thus the observed selectivity is thermodynamic rather than kinetic in origin. Most likely, the ligand **4d** adopts that configuration (D or L) which is most compatible with the antipode of $Ru(bpy)_2Cl_2$ to which it has become associated. This conformational adaptation is facilitated by coordination, which lowers the energy barrier for this process. Future studies will address the possible influence of such chiral ligands on stereochemistry at the metal center. For example, can the barrier for pseudorotation in metal complexes be lowered by the involvement of chiral ligands?

Experimental Section

Nuclear magnetic resonance spectra were recorded on a Nicolet NT-300 WB spectrometer in CD_3CN with chemical shifts reported in parts per million downfield from Me_4Si. Electron absorption spectra were

(10) Rillema, D. P.; Jones, D. S. *J. Chem. Soc., Chem. Commun.* **1979**, 849.

(11) Maspero, F.; Ortaggi, G. *Ann. Chim. (Rome)* **1974**, *64*, 115.

Table VII. X-ray Data Collection and Processing Parameters for **4d**

mol formula	$RuP_2F_{12}ON_6C_{34}H_{32}$	abs coeff	$\mu = 6.03$ cm^{-1}
fw	931.67	radiation (Mo Kα)	$\lambda = 0.71073$ Å
space group	$P\bar{1}$, triclinic	collcn range	$4° \leq 2\theta \leq 36°$
cell constants	$a = 12.485$ (3) Å	scan width	$\Delta\theta = (1.10 + 0.35 \tan\theta)°$
	$b = 12.492$ (7) Å	max scan time	180 s
	$c = 12.563$ (3) Å	scan speed range	0.6–5.0°/min
	$\alpha = 96.91$ (3)°	no. of tot. data collcd	1906
	$\beta = 109.80$ (2)°	no. of indep data, $I > 3\sigma(I)$	1484
	$\gamma = 90.44$ (3)°	no. of total variables	300
	$V = 1827$ Å^3	$R = \sum\|\|F_o\| - \|F_c\|\|/\sum\|F_o\|$	0.058
formula units/cell	$Z = 2$	$R_w = [\sum w(\|F_o\| - \|F_c\|)^2/\sum w\|F_o\|^2]^{1/2}$	0.061
density	$\rho = 1.69$ g/cm^3	weights	$w = \sigma(F)^{-2}$

recorded on a Perkin-Elmer 330 spectrophotometer. Elemental analyses were performed by the Canadian Microanalytical Service, Ltd., New Westminster, BC, Canada. The preparation of the ligands has been previously described.[4] *cis*-$(bpy)_2RuCl_2 \cdot 2H_2O$ was prepared according to a procedure described by Meyer and co-workers.[12]

Cyclic voltammograms were recorded with a PAR Model 174A polarographic analyzer, a PAR Model 175 universal programmer, and a Houston Instruments Omnigraphic 2000 X-Y recorder. A three-electrode system was employed, consisting of a platinum-button working electrode, a platinum-wire auxiliary electrode, and a saturated calomel reference electrode. The reference electrode was separated from the bulk of the solution by a cracked glass bridge filled with 0.1 M tetra-*n*-butylammonium perchlorate (TBAP) in acetonitrile. Deaeration of all solutions was performed by passing high-purity nitrogen through the solution for 5 min and maintaining a blanket of nitrogen over the solution while the measurements were made. Reagent grade acetonitrile was distilled twice from P_2O_5 under nitrogen. The supporting electrolyte, TBAP, was recrystallized from EtOAc/hexane, dried, and stored in a desiccator. Emission spectra were obtained at 298 K on a Perkin-Elmer LS-5 fluorometer at the Center for Fast Kinetics, Austin, TX. Low-temperature emission spectra were obtained on an apparatus that has been described previously.[13]

Preparation of RuL_3^{2+} Complexes. A mixture of 1 equiv of $RuCl_3 \cdot 3H_2O$ and 3.5 equiv of the ligand L in 50% aqueous ethanol was refluxed under nitrogen for periods ranging from 4 to 48 h. After cooling, a solution of 2 equiv of NH_4PF_6 in 5 mL of H_2O was added to precipitate the complex, which was collected, dried, and chromatographed on 20–30 g of neutral alumina with 1:1 toluene–acetonitrile as the eluent. Fractions of 20 mL were collected, and those fractions containing the desired complex as indicated by TLC were allowed to stand at room temperature for 2–3 days, during which time the slow evaporation of acetonitrile caused the pure complex to crystallize. The yields and combustion analyses are summarized in Table VI.

Preparation of $Ru(bpy)_2L^{2+}$ Complexes. The same procedure was followed as outlined above for RuL_3, using *cis*-$(bpy)_2RuCl_2 \cdot 2H_2O$ and ligand L in a molar ratio of 1:1.2. The yields and combustion analyses are summarized in Table VI.

X-ray Determination. A large reddish brown prismatic plate having dimensions 0.50 × 0.40 × 0.15 mm was mounted on a glass fiber in a random orientation on an Enraf-Nonius CAD-4 automatic diffractometer. The radiation used was Mo Kα monochromatized by a dense graphite crystal assumed for all purposes to be 50% imperfect. The Laue symmetry was determined to be 1, and the space group was shown to be either $P1$ or $P\bar{1}$. Intensities were measured by using the θ–2θ scan technique, with the scan rate depending on the net count obtained in rapid prescans of each reflection. Data in the hemisphere of reciprocal space having $h \geq 0$ were collected. Two standard reflections were monitored periodically during the course of the data collection as a check of crystal stability and electronic reliability, and one of them decayed by 20% while the other remained constant. No reasonable correction for this anisotropic decay could be made, and so the data collection was stopped prematurely. In the data reduction, Lorentz and polarization factors were applied; however, no correction for absorption was made due to the small absorption coefficient. No extinction correction was made.

The structure was solved by the Patterson method, which revealed the position of the Ru atom. The remaining non-hydrogen atoms were located in subsequent different Fourier syntheses. The usual sequence of isotropic and anisotropic refinement was followed, after which all hydrogens were entered in ideally calculated positions. Due to the relatively small amount of observed data, only the Ru, P, and F atoms were refined anisotropically. At this point, a large amount of residual electron density indicated the presence of a solvent molecule, assumed to be water. In order for the oxygen temperature factor to refine to a reasonable value, the occupancy factor had to be fixed at 50%; however, this is probably more indicative of partial loss during the course of the data collection

Table VIII. Positional Parameters and Their Estimated Standard Deviations (in Parentheses)

atom	x	y	z
Ru	0.2210 (1)	0.21604 (9)	0.37814 (9)
P1	0.3865 (4)	0.7855 (3)	−0.1170 (4)
P2	0.0870 (5)	−0.3199 (4)	−0.3081 (4)
F1	0.4127 (9)	0.6657 (7)	−0.1233 (9)
F2	0.348 (1)	0.9023 (8)	−0.1172 (9)
F3	0.438 (2)	0.802 (1)	0.005 (1)
F4	0.325 (1)	0.771 (1)	−0.246 (1)
F5	0.4872 (9)	0.8125 (9)	−0.150 (1)
F6	0.275 (1)	0.753 (1)	−0.106 (1)
F7	0.1255 (9)	−0.3054 (9)	0.2026 (7)
F8	0.155 (1)	−0.216 (1)	0.370 (1)
F9	0.058 (1)	−0.3386 (9)	0.4152 (8)
F10	0.021 (1)	−0.4312 (9)	0.2438 (9)
F11	−0.021 (1)	−0.2661 (9)	0.255 (1)
F12	0.192 (1)	−0.390 (1)	0.3555 (9)
N1	0.3610 (9)	0.2977 (7)	0.3733 (7)
N2	0.1465 (9)	0.3087 (8)	0.2491 (8)
N3	0.2126 (9)	0.0951 (8)	0.2454 (8)
N4	0.0763 (9)	0.1322 (8)	0.3616 (8)
N5	0.2204 (9)	0.3279 (8)	0.5120 (8)
N6	0.3028 (9)	0.1394 (8)	0.5140 (8)
C1	0.469 (1)	0.298 (1)	0.444 (1)
C2	0.554 (1)	0.365 (1)	0.444 (1)
C3	0.528 (1)	0.442 (1)	0.376 (1)
C4	0.421 (1)	0.451 (1)	0.303 (1)
C5	0.339 (1)	0.3686 (9)	0.294 (1)
C6	0.226 (1)	0.3539 (9)	0.212 (1)
C7	0.191 (1)	0.376 (1)	0.098 (1)
C8	0.079 (1)	0.370 (1)	0.038 (1)
C9	−0.004 (1)	0.339 (1)	0.079 (1)
C10	0.039 (1)	0.304 (1)	0.186 (1)
C11	0.392 (1)	0.549 (1)	0.240 (1)
C12	0.414 (1)	0.546 (1)	0.128 (1)
C13	0.318 (1)	0.496 (1)	0.028 (1)
C14	0.280 (1)	0.386 (1)	0.038 (1)
C15	0.294 (1)	0.088 (1)	0.193 (1)
C16	0.278 (1)	0.010 (1)	0.100 (1)
C17	0.182 (1)	−0.060 (1)	0.069 (1)
C18	0.102 (1)	−0.052 (1)	0.121 (1)
C19	0.119 (1)	0.028 (1)	0.216 (1)
C20	0.043 (1)	0.049 (1)	0.279 (1)
C21	−0.058 (1)	−0.014 (1)	0.253 (1)
C22	−0.126 (2)	0.012 (1)	0.316 (1)
C23	−0.092 (2)	0.096 (1)	0.401 (1)
C24	0.006 (1)	0.155 (1)	0.422 (1)
C25	0.169 (1)	0.421 (1)	0.501 (1)
C26	0.176 (1)	0.494 (1)	0.598 (1)
C27	0.226 (1)	0.465 (1)	0.701 (1)
C28	0.278 (1)	0.369 (1)	0.713 (1)
C29	0.275 (1)	0.298 (1)	0.618 (1)
C30	0.327 (1)	0.196 (1)	0.618 (1)
C31	0.383 (1)	0.151 (1)	0.717 (1)
C32	0.421 (1)	0.051 (1)	0.709 (1)
C33	0.398 (1)	−0.007 (1)	0.607 (1)
C34	0.342 (1)	0.039 (1)	0.510 (1)
O1	0.356 (2)	0.828 (2)	0.322 (2)

(12) Sullivan, B. P.; Salmon, D. J.; Meyer, T. J. *Inorg. Chem.* **1978**, *17*, 3334.
(13) Waddell, W. H.; Schaffer, A. M.; Becker, R. S. *J. Am. Chem. Soc.*, **1973**, *95*, 8223.

rather than true disorder. Hydrogen isotropic temperature factors were estimated on the basis of the thermal motion of the associated carbons. After all shift:esd ratios were less than 0.3, convergence was reached. No unusually high correlations were noted between any of the variables in the last cycle of least-squares refinement, and the final difference density map showed no peaks greater than 0.25 e/Å^3. The atomic scattering factors for the non-hydrogen atoms were computed from numerical Hartree–Fock wave functions;[14] for hydrogen those of Stewart, Davidson, and Simpson[15] were used. The anomalous dispersion coefficients of Cromer and Liberman[16] were used for Ru. All calculations were made by using Molecular Structure Corp. TEXRAY 230 modifications of the SDP-PLUS series of programs. The data collection and processing parameters are outlined in Table VII, and the positional parameters and their standard deviations are included in Table VIII.

Acknowledgment. Financial support from the Robert A. Welch Foundation and the donors of the Petroleum Research Fund, administered by the American Chemical Society, is gratefully acknowledged. F.L. also wishes to acknowledge support from a Stella Erhardt Memorial Fellowship and a Grant-in-Aid of Research from Sigma Xi, the Scientific Research Society. We thank Prof. Ralph Becker for assistance in obtaining the emission spectra.

Supplementary Material Available: Tables pertinent to the X-ray crystallographic determination of **4d** including bond lengths, bond angles, refined and general temperature factor expressions, least-squares planes, and calculated hydrogen fractional coordinates (8 pages); a listing of observed and calculated structure factors (8 pages). Ordering information is given on any current masthead page.

(14) Cromer, D. T.; Mann, J. B. *Acta Crystallogr., Sect. A: Cryst. Phys., Diffr., Theor. Gen. Crystallogr.* **1968**, *A24*, 321.
(15) Stewart, R. F.; Davidson, E. R.; Simpson, W. T. *J. Chem. Phys.* **1965**, *42*, 3175.
(16) Cromer, D. T.; Liberman, D. *J. Chem. Phys.* **1970**, *53*, 1891.

Contribution from the Departments of Chemistry, State University Groningen, 9747 AG Groningen, The Netherlands, and Leiden University, 2300 RA Leiden, The Netherlands

Crystal Structure, Electron Spin Resonance, and Magnetic Exchange Coupling in Bis(μ-chloro)bis[cyclopentadienyl(triethylphosphane)vanadium(II)]

J. Nieman,[1a] J. H. Teuben,*[1b] F. B. Hulsbergen,[1c] R. A. G. de Graaff,[1c] and J. Reedijk[1c]

Received November 26, 1986

The X-ray structure and magnetic characterization (ESR, susceptibility) of the dinuclear vanadium(II) compound $[CpVCl(PEt_3)]_2$ are described. The title compound crystallizes in the monoclinic space group as purple-red crystals, with cell dimensions of a = 12.760 (5) Å, b = 12.616 (7) Å, c = 17.707 (7) Å, and β = 102.32 (3)°, in space group $P2_1/c$, with Z = 4. The structure was solved by using Mo Kα radiation (λ = 0.71073 Å) and 7090 reflections (3607 unique intensities, 1390 of which were considered as observed), resulting in $R(F)$ = 0.0589 ($R_w(F)$ = 0.0458). The structure consists of roof-shaped dinuclear V_2Cl_2 units and terminal η^5-cyclopentadienyl and triethylphosphane ligands. The V–V distance amounts to 3.245 (3) Å. The bridge, though roof-shaped (dihedral angle of 132.9°), is quite symmetric as deduced from V–Cl distances of 2.438 (3) and 2.440 (3) Å. The dimeric unit results in antiferromagnetic interaction between the two V(II) (d^3) ions, as seen from ESR spectra and magnetic susceptibility studies at low temperature.

Introduction

The chemistry of vanadium(II) is poorly developed,[2,3] and only a relatively small number of coordination compounds have been described in great detail by X-ray structure analysis. Apart from coordination compounds of the type V(ligand)$_6$X$_2$ and V(ligand)$_4$X$_2$ (X = halide; L = (heterocyclic) nitrogen donor ligand),[4] vanadium(II) Tutton salts,[5] and cationic dinuclear V(II) complexes, $[V_2(\mu\text{-}X)_3(THF)_6]^+$,[6] mostly organometallic V(II) species have been described,[7] often by using THF salts as intermediates. In earlier studies[6-8] it turned out that cyclopentadienyl V(III) compounds of formula $CpVX_2(L)_2$ (L = phosphane-type ligand; X = Cl, Br) are easily reduced to species analyzing as CpVCl(L). Extensive characterization by a variety of physical methods in solution strongly indicates that these species are dimeric in nature with halogen-bridged dinuclear species, just as has been reported before[6] for $[V_2X_3(THF)_6]^+$ species.

The present paper describes the characterization of one of these compounds by X-ray methods, as well as a study of the dinuclear species by means of ESR spectroscopy and magnetic susceptibility measurements.

Table I. Crystal and Diffraction Data for $[CpVCl(PEt_3)]_2$

empirical formula	$C_{22}H_{40}Cl_2P_3V_2$
color	purple red
cryst dimens, mm	0.22 × 0.15 × 0.10
space group	$P2_1/c$
cell dimens (at 25 °C; 24 reflctns; 12° < θ < 15°)	
a, Å	12.760 (5)
b, Å	12.616 (7)
c, Å	17.707 (7)
β, deg	102.32 (3)
θ values, deg	$4 < \theta < 44$
molecules/cell	4
V, Å^3	2784.8
d_{calcd} g/cm^3	1.284
wavelength Mo Kα_1, Å	0.71073
M_r	539.30
linear abs coeff, cm^{-1}	9.65
total no. of reflcns collcd	7090
no. of unique intens	3607 (R_{int} = 0.058)
final residuals	
$R(F)$	0.0589
$R_w(F)$ ($w = 1/\sigma^2(F)$)	0.0458
goodness of fit for the last cycle(s)	1.75
max Δ/σ for the last cycle	<0.1

Experimental Section

The compounds studied are extremely air sensitive, and experiments were carried out under rigorously anhydrous and oxygen-free conditions. Solvents (toluene, ether, pentane) were distilled under nitrogen from sodium/potassium melts before use. The compound $[CpVCl(PEt_3)]_2$ was prepared as reported before.[7]

(1) (a) Present address: AKZO Chemie Nederland b.v., 1000 AA Amsterdam, The Netherlands. (b) State University Groningen. (c) Leiden University.
(2) Cotton, F. A.; Wilkinson, G. *Advanced Inorganic Chemistry*, 4th ed., Wiley: New York, 1980.
(3) Mani, F. *Inorg. Chim. Acta* **1980**, *38*, 97.
(4) Larkworthy, L. F.; O'Donoghue, M. W. *Inorg. Chim. Acta* **1983**, *71*, 81.
(5) Patel, K. C.; Goldberg, D. E. *J. Chem. Educ.* **1973**, *50*, 868.
(6) Bouma, R. J.; Teuben, J. H.; Beukema, W. R.; Bansemer, R. L.; Huffmann, J. C.; Caulton, K. G. *Inorg. Chem.* **1984**, *23*, 2715.
(7) Nieman, J.; Teuben, J. H.; Huffmann, J. C.; Caulton, K. G. *J. Organomet. Chem.* **1983**, *255*, 193.
(8) Nieman, J.; Teuben, J. H. *Organometallics* **1986**, *5*, 1149.

0020-1669/87/1326-2376$01.50/0